

Nanopore arrays in a silicon membrane for parallel single-molecule detection: DNA translocation

This content has been downloaded from IOPscience. Please scroll down to see the full text.

2015 Nanotechnology 26 314002

(<http://iopscience.iop.org/0957-4484/26/31/314002>)

View [the table of contents for this issue](#), or go to the [journal homepage](#) for more

Download details:

IP Address: 130.237.214.51

This content was downloaded on 24/07/2015 at 10:35

Please note that [terms and conditions apply](#).

Nanopore arrays in a silicon membrane for parallel single-molecule detection: DNA translocation

Miao Zhang¹, Torsten Schmidt¹, Anders Jemt², Pelin Sahlén², Ilya Sychugov¹, Joakim Lundberg² and Jan Linnros¹

¹ Materials and Nano Physics, School of Information and Communication Technology, KTH Royal Institute of Technology, Electrum 229, SE-16440 Kista-Stockholm, Sweden

² Science for Life Laboratory, School of Biotechnology, KTH Royal Institute of Technology, SE-17165 Solna-Stockholm, Sweden

E-mail: miaoz@kth.se and linnros@kth.se

Received 10 March 2015, revised 24 April 2015

Accepted for publication 2 June 2015


Published 16 July 2015



CrossMark

Abstract

Optical nanopore sensing offers great potential in single-molecule detection, genotyping, or DNA sequencing for high-throughput applications. However, one of the bottle-necks for fluorophore-based biomolecule sensing is the lack of an optically optimized membrane with a large array of nanopores, which has large pore-to-pore distance, small variation in pore size and low background photoluminescence (PL). Here, we demonstrate parallel detection of single-fluorophore-labeled DNA strands (450 bps) translocating through an array of silicon nanopores that fulfills the above-mentioned requirements for optical sensing. The nanopore array was fabricated using electron beam lithography and anisotropic etching followed by electrochemical etching resulting in pore diameters down to ~ 7 nm. The DNA translocation measurements were performed in a conventional wide-field microscope tailored for effective background PL control. The individual nanopore diameter was found to have a substantial effect on the translocation velocity, where smaller openings slow the translocation enough for the event to be clearly detectable in the fluorescence. Our results demonstrate that a uniform silicon nanopore array combined with wide-field optical detection is a promising alternative with which to realize massively-parallel single-molecule detection.

 Online supplementary data available from stacks.iop.org/NANO/26/314002/mmedia

Keywords: nanopore, parallel, single-molecule, optical

Introduction

Since the completion of the human genome sequencing project approximately 15 years ago, the demands for fast sequencing techniques have driven a race towards parallel DNA sequencing methods [1] with the goal of achieving full genome mapping within a few hours (the '\$1000 genome' [2]). This has lately been fueled by the need for rapid DNA sequencing of samples from individual patients since it has been realized that the outcome of many medications is dependent on local variations of human genes. Such 'personalized medicine' has called for inexpensive, massively-parallel sequencing methods, where miniaturization using current

silicon processing nanotechnology seems a viable route. A concept that has attracted much interest here is to employ a solid-state membrane containing a nanopore array through which single DNA strands would translocate. The read-out of the sequence of the DNA, encoding the genes, could then be performed electrically using the changes of the ionic current through the pore when the DNA molecule passes inside the pore [3]. Clearly, for this concept to be effective, the nanopores must be in the ~ 2 nm diameter range with a very small variation in size and the membrane thickness has to reach sub-nm range since the distance between adjacent bases is only 0.34 nm. Furthermore, the electrical read-out must be fast and accurate enough to distinguish individual bases. Apart from

DNA sequencing, the nanopore concept could have many other applications such as single-molecule sensing, size selection and specific biomolecule detection using functionalized pores.

While most of the publications dealing with SiN membranes with a single nanopore prepared by focused electron beam or ion beam drilling report on electrical read-out [4–8], it has been suggested that optical read-out using fluorophores attached to the DNA would enable a safer discrimination of the base sequence relaxing also the need for separate electrodes for reading the ionic current associated to each nanopore [9, 10]. Having an array of well-separated nanopores, optical read-out allows parallel simultaneous detection of translocation events using fast camera techniques and thus high analyte throughput. To address the fast translocation speed and to enable read-out using only two fluorophores, Amit Meller [9] proposed an attractive approach using a binary scheme conversion of the original DNA strand. This was demonstrated using single drilled SiN nanopores, but has not been shown for large arrays of nanopores where drilling is an inherently slow process. Other challenges related to this relatively new concept include achieving uniform arrays with small variations in pore size and low background photoluminescence from the membrane itself [24]. The latter requirement is a serious problem as the silicon nitride membranes that are mostly in use today have been reported to have PL emission in the range of 500 to 900 nm [11, 12], where commonly used fluorophores are emitting. Thus, the PL background from the membrane lowers the sensitivity of the read-out and single-fluorophore detection may become impossible. Another limiting factor for massively-parallel optical nanopore sensing is the relatively slow read-out rate of CCD cameras in comparison to the fast DNA translocation through a pore. For confocal or total internal reflection fluorescence (TIRF) microscopy, which is typically used in nanopore sensing experiments, the detection volume is so small that only a very short detection window in time is available for the camera.

Here we report on DNA translocation experiments through an array of nanopores fabricated in a silicon membrane. The membrane was fabricated using silicon processing technology and an array of nanopores was obtained by using electron-beam lithography, anisotropic etching and electrochemical etching. This resulted in regularly-spaced nanopores with diameters down to ~ 7 nm in a 300 nm thick membrane, as described in a companion paper [13]. While the location of the pore is set by lithography, the pore diameter is controlled by etching bias and current. The high aspect ratio of the pores is believed to slow down the translocation velocity of DNA [14, 15]. In this paper we focus on using such arrays of silicon nanopores for parallel detection of DNA translocation in a conventional wide-field microscope. The low background PL, inherent in the silicon membrane, the high aspect ratio of the pores and the relatively large depth of focus of the microscope used here allow us for the first time to detect parallel single-fluorophore-labeled DNA translocations through 20–30 nm pores using a wide-field microscope with an electron-multiplying CCD camera.

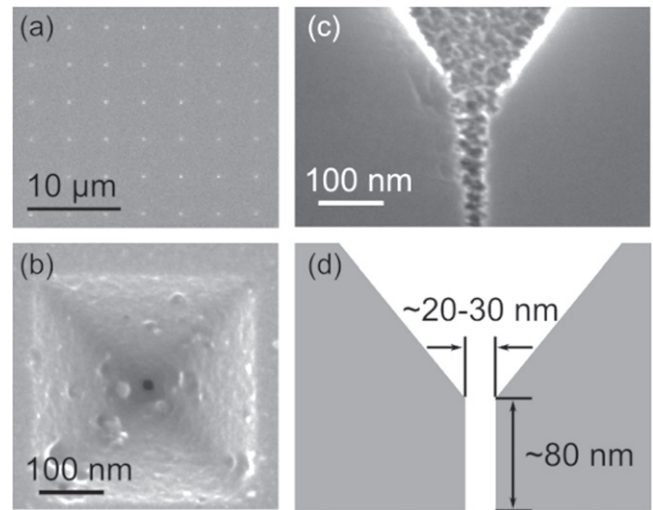


Figure 1. (a) A SEM image of a nanopore array with a pitch distance of $4\ \mu\text{m}$ on a silicon membrane. (b) A SEM top view of a nanopore with a diameter of 20 nm, which is located in the center of an inverted pyramid. The surface of the inverted pyramid was partly roughened during the etching. (c) Cross-sectional view of a electrochemically etched nanopore in bulk silicon. (d) A schematic cross-section of a nanopore on a silicon membrane. The top inverted pyramidal structure is fabricated by KOH etching, while the pore at the bottom is formed by electrochemical etching in HF.

Experimental details

A wafer of chips containing 300 nm thick silicon membranes with arrays of inverted pyramidal structure was fabricated by standard cleanroom processing [16]. Each chip was 1.5×1.5 cm in size and contained 32 membranes. Nanopores were then formed by electrochemical etching of silicon in hydrofluoric acid (HF). During electrochemical etching, silicon is dissolved in the electrolyte (HF) owing to the exchange of charge carriers at the silicon-electrolyte interface under bias. Pores are formed at the tip of the inverted pyramids due to positive charge carriers attracted by the higher local electric field. Details on the fabrication process, including a description of the etching parameters, can be found in a companion paper [13]. With respect to this fabrication method, membranes with 10 by 10 pore arrays were selected and prepared for further DNA translocation experiments. The membranes were characterized by scanning electron microscopy (SEM; Gemini, ULTRA55, Zeiss). A SEM image of such an array of nanopores with a pitch distance of $4\ \mu\text{m}$ is shown in figure 1(a). It was found that the diameters of the pores are mainly between 20 to 30 nm, with a few exceptions as large as a couple of hundred nanometers. Smaller diameters down to ~ 7 nm can also be achieved although not used for translocation experiments here. Figure 1(b) shows a representative pore with a diameter of 20 nm in top view. Due to the difficulty of obtaining a cross-sectional view of a nanopore on a membrane, a SEM cross-section of a nanopore, fabricated also by electrochemical etching in bulk silicon, is shown in figure 1(c). It can be seen that the pore wall is upright. The effective pore depth is defined as the distance between the pore opening at the bottom of the etching pit and the backside

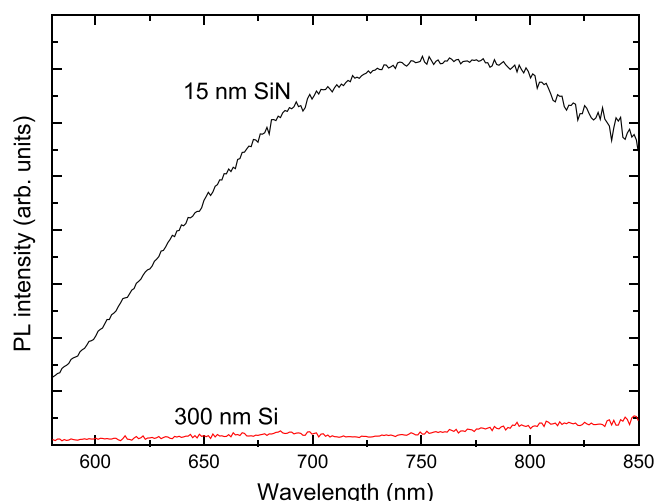


Figure 2. Photoluminescence spectra of a SiN membrane (black) and a Si membrane (red). The 15 nm thick SiN and the 300 nm thick Si free-standing membranes were excited by a 514 nm laser. The PL spectra were recorded under the same conditions to permit comparison. While the SiN membrane shows a strong emission from 580 to 850 nm, the PL emitted by the Si membrane is negligible.

of the membrane. Since the inverted pyramids were formed by anisotropic KOH etching, the depth of the pyramid is $1/\sqrt{2}$ of the width. Therefore, we estimated that the effective depth of the pore is around 80 nm; see figure 1(d). The aspect ratio of these electrochemically etched pores can be as high as 4, while the one for TEM-drilled pores is typically around 1 [17–19]. Further, to characterize the optical properties of the membrane, photoluminescence micro-spectroscopy was performed respectively on a 300 nm thick Si membrane and on a 15 nm thick SiN membrane (TED PELLA, INC.) under the excitation of a 514 nm Omicron Phoxx diode laser. The spectra were obtained by an imaging spectrometer (Andor Shamrock 500), which was connected to an inverted microscope. An electron-multiplying CCD (EMCCD) camera (Andor iXon-X3 888) was used to record the signal. All measurements were performed under the same conditions with the laser focused at the center of the membrane. As shown in figure 2, the SiN membrane has a relatively intense and broad PL emission covering 580 to 850 nm, even though the thickness of the membrane is 15 nm only. On the contrary, the 300 nm thick Si membrane reveals negligible PL in the same wavelength range. The low PL of bulk Si in the visible range is attributed to its small energy bandgap, which is 1.11 eV at 300 K.

For the DNA translocation experiments, a membrane with a pitch distance of $8\ \mu\text{m}$ was selected. After oxygen-plasma treatment to increase the surface wettability, the membrane chip was mounted on a home-made double cell with cis- and trans-chambers as shown in figure 3. A PDMS sheet with a single channel was added to the backside of the chip to allow only one membrane being exposed to the buffer solution. The buffer, a diluted saline-sodium citrate (SSC) solution (10 mM NaCl, 1 mM sodium citrate, pH = 7.0), was filled in both chambers and in-house synthesized 450 bps double-strand (ds) DNA labeled with single fluorophores

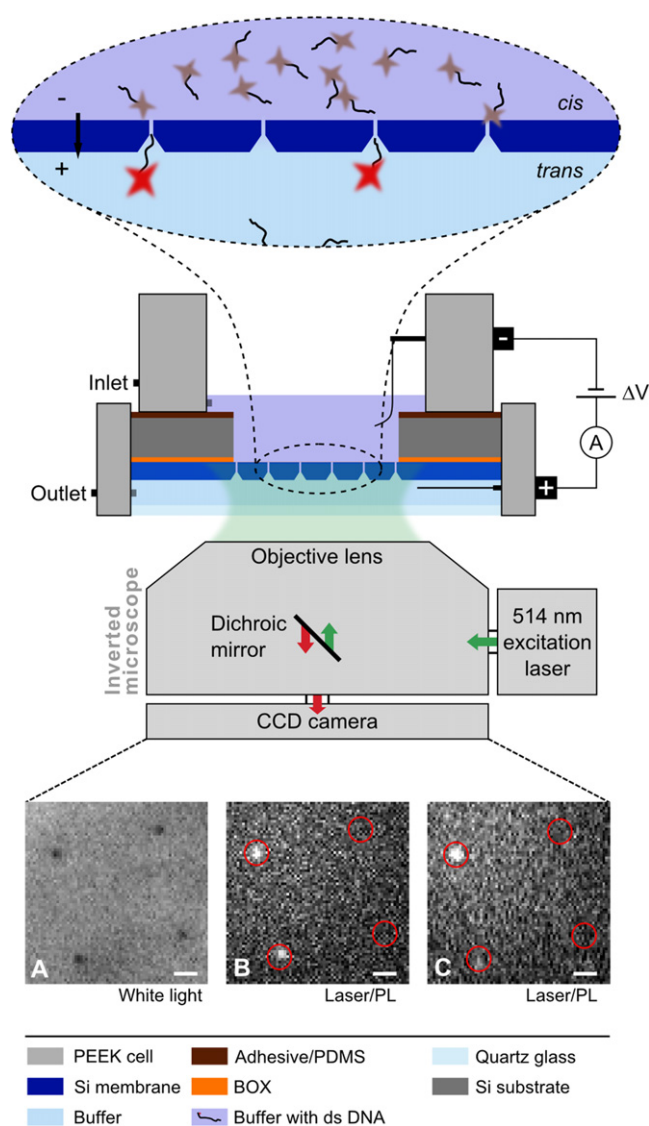


Figure 3. Optical detection of translocation events. Middle: scheme (not to scale) of the sequencing cell (PEEK: polyether ether ketone) designed for optical read-out using an inverted microscope. Top: zoom-in shows scheme of translocation of double stranded DNA strings labeled with a fluorophore (star-like symbol). Bottom left: white light reflection image of 4 pores located in a 10×10 array with $8\ \mu\text{m}$ pore-to-pore distance. Bottom right: two frames from a sequence of photoluminescence images of the same area. The scale bars in image (a), (b) and (c) are $2\ \mu\text{m}$.

(Atto-532) were added to the cis-chamber. The final concentration of the analyte in the cis-chamber was no more than 100 pM. A bias of 1 V was applied across the membrane to drive DNA through the nanopores, while a sequence of images being recorded. Details about the DNA synthesis can be found in the supplementary information.

As illustrated in figure 3, the detection cell was placed on top of an inverted wide-field microscope with bright-field laser excitation (514 nm). The laser, operated at 60 mW, is focused on the membrane with a spot area of $75\ \mu\text{m}^2$, which results in a power density of $4.6 \times 10^4\ \text{W cm}^{-2}$. Such high excitation is used to maximize the signal-to-noise ratio. Considering the fact that optical read-out is performed at a

single molecule level, effective background PL control is critical, in particular under bright-field excitation using a wide-field microscope. To avoid Raman scattering from water molecules here at the wavelength of 625 nm, a bandpass filter at 571/72 nm was used as emission filter. A dichroic mirror and a single bandpass filter at 514/3 nm as excitation filter eliminate the backscattered excitation light as a background source. A thin quartz window, instead of normal glass, with a thickness of 170 μm is mounted as closing on the trans-chamber in order to minimize the background PL. A 63x objective lens with window correction is used to compensate the image distortion induced by the quartz window and the liquid in the cell. In this configuration, the optical signal emitted at the nanopore region, passes the beamsplitter cube, and is then collected by the EMCCD. The actual field of view is cropped to approximately $50 \times 50 \mu\text{m}^2$ in order to increase the frame rate. On a nanopore array with a pore-to-pore distance of 8 μm , 30 pores were imaged at the same time. With an acquisition time of 50 ms for each image and a read-out time of ~ 50 ms, the total frame acquisition rate is ~ 10 Hz.

Results and discussion

An example of recorded PL images is shown in the lower panel of figure 3. Here, a white light image of 2×2 pores and 2 frames from a sequence of PL images, that captured translocation events, are shown. The dark points in the white light image, which are actually the inverted pyramids, indicate the pore locations. In the PL images the white spots represent translocations of DNA molecules. The intensity of these successive PL signals was extracted as a function of time for several individual pores from a sequence of recorded images by using the software ImageJ with a home-built Java code.

A set of simultaneously recorded intensity time traces, where the pore diameter varies from 20 to 440 nm, is shown in figure 4. Observing the time-dependent signal, it is obvious that the three small pores (20, 30 and 32 nm) reveal similar time traces with well distinguishable, repeating PL peaks, indicating frequent translocation events, while interestingly the larger pores (370, 440 nm) show clearly different behavior. Taking into account that the raw data was recorded within several hours and was obtained from pores located on the same membrane, environmental conditions (such as local buffer concentration, temperature gradient due to laser, etc) of these pores can be considered as almost identical. Thus, we rather assume that the differences of translocation behavior for different pores can be attributed to diameter and geometry. To gain more insight into the translocation mechanism, further analyses of the intensity time traces were done with respect to the latter point.

Intensity histograms corresponding to the traces above (after background subtraction) are shown in figures 5(a)–(c) for the pores with a diameter of 32, 370 and 440 nm, respectively. The Gaussian fit (truncated orange curve peaking around zero) represents the background signal, where the standard deviation σ of approximately 100 counts is the

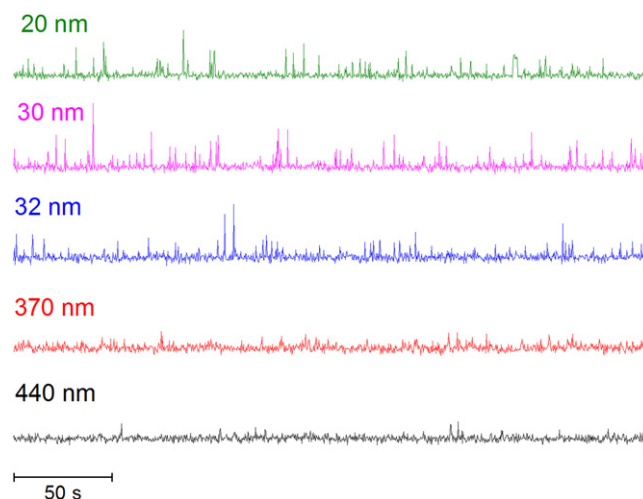


Figure 4. Photoluminescence intensity time traces at the location of individual pores, obtained on an array of pores with diameters ranging from 20 to 440 nm, under a bias of 1 V.

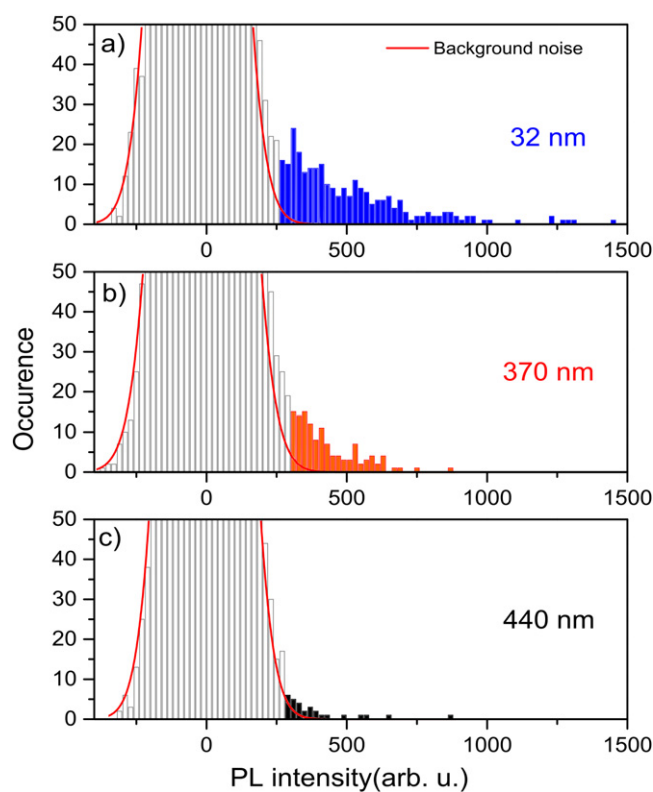


Figure 5. Intensity histograms of translocation recorded at nanopores with diameters of 32, 370 and 440 nm, respectively. Gaussian fittings (orange) of the background signal are displayed on top of the histograms. PL signals which are larger than 3σ over the background are counted as translocation events, which are colored.

background noise level for all three pores. Intensity values exceeding 3σ of the background signal are set to be counted as translocation events (colored counts). From this plot, a clear dependency on the pore diameter can be observed, i.e. the number of detected events increases with decreasing pore diameter. Based on the on/off threshold, being set also at 3σ of the background signal, the statistics of translocation

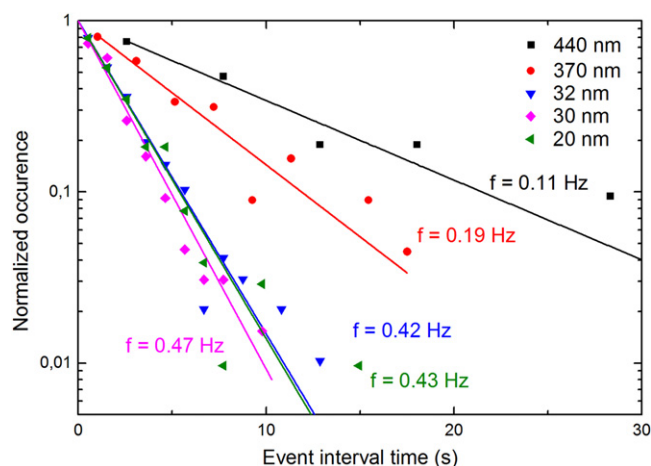


Figure 6. Normalized event interval time (off-time) distributions. The event interval time distribution falls off inversely with the pore diameter.

duration (on-time, see supporting information figure S1) and event rate (off-time) can be further extracted. The event rate distribution, shown in figure 6 in a (normalized) semi-log plot, can be fitted well with a single exponential function, which implies that most likely single-molecule events are detected and that the process that a molecule finds and passes through a pore is purely random. The characteristic event rate is directly obtained from the decay constant of the mono-exponential function. For example the event rate of the 30 nm pore is 0.47 ± 0.02 Hz, which is way below the frame rate (10 Hz). At such event rate regime, we believe that the most events of the arising in PL intensity at the pore positions are resulted from single molecules. Now let us focus on the event rate of pores with different diameters. Described by the Smoluchowski rate equation [20]

$$J = 2\pi c D r_p,$$

with constant analyte concentration (c) and diffusion coefficient (D), the rate of analytes (J) arriving at the pore entrance governed by free diffusion should scale linearly with the pore diameter ($2r_p$). Surprisingly, it is found in our detection that the event rate scales inversely with the pore diameter. For example the 370 nm pore has an event rate of 0.19 ± 0.02 Hz only. By the Smoluchowski rate equation, we estimated the arriving rate of DNA is 0.05 Hz for a 30 nm pore, and 0.61 Hz for a 370 nm pore. The detected event rate on the small pores (20–32 nm) is on average almost 10 times greater than the Smoluchowski rate, which is in agreement with the results reported by other groups, when bias is applied [20]. On the other hand, one would expect that larger pores allow more molecules to pass per unit time, resulting in a higher event rate and even multi-molecule events with higher PL intensity. However, the experimental results clearly show the opposite. This discrepancy, i.e. the ‘missing’ events on the larger pores, will be discussed in the following section.

First, it should be emphasized that the optical detection mechanism used here substantially differs from electrical

detection or other optical detection using confocal or TIRF microscopy, typically used in such experiments. Under the continuous laser excitation, fluorophores are detectable by the CCD camera within the entire depth of focus of the objective lens. In a wide-field microscope, a 63x objective lens has a depth of focus of $\sim 1 \mu\text{m}$, which is about 50 times larger than the thickness of the pores used in electrical measurements, or 10 times larger than the depth of focus of a confocal microscopy or the evanescent field in TIRF microscopy. As an example, the time it takes for a 450 bps DNA to diffuse through such distance is calculated. The diffusion coefficient of a 450 bps DNA, as used in our experiments, can be estimated as $9.2 \times 10^{-12} \text{ m}^2 \text{ s}^{-1}$ [21]. Thus, the time anticipated for such a molecule to move through the depth of focus purely by diffusion is around 110 ms. Following this, the event duration for optical detection should be significantly longer than the dwell-time measured by ionic current blockage, which is typically within 1 ms (for DNA of a length less than 1 kbps passing through a ~ 10 nm pore) [7, 19–23]. Note that this fact of significantly longer event durations allowed us to use wide-field microscope optical detection with an acquisition frame rate of about 10 Hz only.

However, when a bias is applied, a recorded translocation event is a combined process of a molecule passing through a pore driven by electro-kinetic forces (electrophoresis and electro-osmosis) [25–27] and moving out of the depth of focus governed by both local electric field and diffusion [28]. Depending on the pore diameter, the electro-kinetic forces and the molecule-pore interaction may accelerate or slow down the whole translocation process, resulting in shorter or longer event durations. In fact, more than 75% of the recorded translocations are single-frame events, indicating that most of the event durations are shorter than the active acquisition time of 50 ms. When the whole translocation process is less than the active acquisition time, the PL intensity is defined by the time that the molecule appears in the detection volume, thus scaling with the translocation time. As already shown in figure 5, the PL intensity distributions of large pores do not have events far above the noise level. Thus, the most probable explanation is that the translocation through the larger pores is too fast to be fully captured by our optical system. In order to have a rough estimation of the detection limit, we considered that the translocation events which last more than two frames reveal the intensity of a single-fluorophore stay-in focus for the entire frame. The average single-fluorophore full-frame PL intensity is ~ 700 counts (see supplementary information, figure S2), while the background 3σ is about 300 counts. Assume the detection limit of our optical system is when signal-to-noise ratio is equal to three, that is, 300 counts. Thus, the detection limit in terms of single molecular translocation time is $\sim 43\%$ of the acquisition time; that is ~ 21 ms in our optical system. As a consequence the event is not detected when the translocation time is shorter than 21 ms.

The small pores, on the other hand, show relatively high event rates. This suggests that the pore diameter can be a limiting factor for the whole event time, although passing

through a pore is only one part of the translocation process. Indeed, studies based on ionic current measurements show that when a molecule–pore interaction contributes to the translocation process, the dwell-time distribution transforms from a Gaussian-shaped curve to a log-normal curve [22]. Enhanced interaction increases the width of the dwell-time distribution resulting in a longer tail [29]. Such transformation is also observed to some extent in the distributions shown in figure 5. Considering the fact that the natural form of a 450 bps dsDNA in 10 mM buffer solution is similar to a loose wool ball with a radius of gyration of 55 nm [21], the DNA molecule has to reshape itself (‘squeeze’) in order to pass a 30 nm pore. Taking into account that the depth of an electrochemically etched pore is about 80 nm, which is several times longer than the depth of TEM-drilled pores (10–20 nm) [30], used in electrical detection schemes, the translocation time is affected probably even stronger in our system by the molecule–pore interaction. Further, the local electric field around a pore is also related to its diameter [28]. Thus, the movement of a DNA molecule in the pore vicinity may also depend on the pore diameter. Synchronized measurements of optical and electrical detection would be useful to further elucidate the translocation process. Nevertheless, we conclude here that slowing down the translocation time allows more events to be detected and thus a higher event rate is observed for the smaller pores. For future experiments, we plan to increase the temporal resolution by using a single-channel avalanche photodiode detector (APD) to investigate the translocation through small pores. Remarkably, the statistics obtained from the small pores with similar diameters (20–32 nm) are quite similar; this indicates that the variation of single molecule detections between pores with similar geometry is small. Thus, the pore arrays fabricated by electrochemical etching are promising to be used in high-throughput parallel sensing. Their high aspect ratio (deep depth) further seems to enable a slowing down of the DNA translocation speed which can be advantageous for accurate optical detection.

Conclusions

In summary, a silicon membrane was found to be a viable alternative for biomolecule optical detection due to its low PL in the visible range. DNA translocation was measured on an array of silicon nanopores, varying in diameter from 20 to 440 nm, by using a wide-field optical microscope. Individual DNA translocation events could be detected simultaneously for several nanopores. Statistical analysis based on discrimination between small (~30 nm) and large (~400 nm) nanopores allowed us to explain the translocation mechanism by electro-kinetic forces and molecule–pore interaction. The observed translocation characteristics make such arrays attractive for single molecule detection as well as for high-throughput parallel biomolecule sensing and DNA sequencing.

Acknowledgments

This project is funded by the Swedish Foundation for Strategic Research through the grant RMA08-0090. Fatemeh Sanghaleh is acknowledged for performing e-beam lithography, Benjamin Bruhn for writing the Java code (ImageJ), Niclas Roxhed for valuable contribution in membrane fabrication and Chonmanart Ngampeerapong for performing electrochemical etching on bulk silicon.

References

- [1] Branton D *et al* 2008 The potential and challenges of nanopore sequencing *Nat. Biotechnol.* **26** 1146–53
- [2] Hayden E C 2014 Technology: the \$1000 genome *Nature* **507** 294–5
- [3] Deamer D W and Akeson M 2000 Nanopores and nucleic acids: prospects for ultrarapid sequencing *Trends Biotechnol.* **18** 147–51
- [4] Storm A J, Chen J H, Ling X S, Zandbergen H W and Dekker C 2003 Fabrication of solid-state nanopores with single-nanometre precision *Nat. Mater.* **2** 537–40
- [5] Wanunu M, Sutin J and Meller A 2009 DNA profiling using solid-state nanopores: detection of DNA-binding molecules *Nano Lett.* **9** 3498–502
- [6] Wu M-Y, Smeets R M M, Zandbergen M, Ziese U, Krapf D, Batson P E, Dekker N H, Dekker C and Zandbergen H W 2009 Control of shape and material composition of solid-state nanopores *Nano Lett.* **9** 479–84
- [7] Kowalczyk S W and Dekker C 2012 Measurement of the docking time of a DNA molecule onto a solid-state nanopore *Nano Lett.* **12** 4159–63
- [8] Carlsen A T, Zahid O K, Ruzicka J A, Taylor E W and Hall A R 2014 Selective detection and quantification of modified DNA with solid-state nanopores *Nano Lett.* **10** 5488–92
- [9] McNally B, Singer A, Yu Z, Sun Y, Weng Z and Meller A 2010 Optical recognition of converted DNA nucleotides for single-molecule DNA sequencing using nanopore arrays *Nano Lett.* **10** 2237–44
- [10] Gilboa T and Meller A 2015 Optical sensing and analyte manipulation in solid-state nanopores *Analyst* **C4AN02388A**
- [11] Sawafta F, Clancy B, Carlsen A T, Huber M and Hall A R 2014 Solid-state nanopores and nanopore arrays optimized for optical detection *Nanoscale* **6** 6991–6
- [12] Assad O N, Fiori N, Di, Squires A H and Meller A 2015 Two color DNA barcode detection in photoluminescence suppressed silicon nitride nanopores *Nano* **15** 745–52
- [13] Schmidt T, Zhang M, Sychugov I, Roxhead N and Linnros J 2015 *Nanotechnology* **26** 314001
- [14] Cabello-Aguilar S, Balme S, Chaaya A A, Bechelany M, Balanzat E, Janot J-M, Pochat-Bohatier C, Miele P and Dejardin P 2013 Slow translocation of polynucleotides and their discrimination by α -hemolysin inside a single track-etched nanopore designed by atomic layer deposition *Nanoscale* **5** 9582–6
- [15] Liu Q, Wu H, Wu L, Xie X, Kong J, Ye X and Liu L 2012 Voltage-driven translocation of DNA through a high throughput conical solid-state nanopore *PLoS One* **7** 1–9
- [16] Zhang M, Schmidt T, Sanghaleh F, Roxhed N, Sychugov I and Linnros J 2014 Oxidation of nanopores in a silicon membrane: self-limiting formation of sub-10 nm circular openings *Nanotechnology* **25** 355302
- [17] Wu M Y, Smeets R M M, Zandbergen M, Ziese U, Krapf D, Batson P E, Nynke H D, Dekker C and Zandbergen H W

- 2009 Control of shape and material composition of solid-state nanopores *Nano Lett.* **9** 479–84
- [18] Kim M J, Wanunu M, Bell D C and Meller A 2006 Rapid Fabrication of uniformly sized nanopores and nanopore arrays for parallel DNA analysis *Adv. Mater.* **18** 3149–53
- [19] Kim M J, McNally B, Murata K and Meller A 2007 Characteristics of solid-state nanometre pores fabricated using a transmission electron microscope *Nanotechnology* **18** 205302–7
- [20] Plesa C, Kowalczyk S W, Zinsmeister R, Grosberg A Y, Rabin Y and Dekker C 2013 Fast translocation of proteins through solid state nanopores *Nano Lett.* **13** 658–63
- [21] Kirby B J 2010 *Micro- and Nanoscale Fluid Mechanics* (Cambridge: Cambridge University Press)
- [22] Wanunu M, Sutin J, McNally B, Chow A and Meller A 2008 DNA translocation governed by interactions with solid-state nanopores *Biophys. J.* **95** 4716–25
- [23] Storm A J, Storm C, Chen J, Zandbergen H, Joanny J-F and Dekker C 2005 Fast DNA translocation through a solid-state nanopore *Nano Lett.* **5** 1193–7
- [24] Chansin G A T, Mulero R, Hong J, Kim M J, DeMello A J and Edel J B 2007 Single-molecule spectroscopy using nanoporous membranes *Nano Lett.* **7** 2901–6
- [25] Luan B, Stolovitzky G and Martyna G 2012 Slowing and controlling the translocation of DNA in a solid-state nanopore *Nanoscale* **4** 1068
- [26] Firnkes M, Pedone D, Knezevic J, Döblinger M and Rant U 2010 Electrically facilitated translocations of proteins through silicon nitride nanopores: conjoint and competitive action of diffusion, electrophoresis, and electroosmosis *Nano Lett.* **10** 2162–7
- [27] Paik K, Liu Y, Tabard-cossa V, Waugh M J, Huber D E, Provine J, Howe R T, Dutton R W and Davis R W 2012 Control of DNA capture by nano fluidic transistors *ACS Nano* **6** 6767–75
- [28] Wanunu M, Morrison W, Rabin Y, Grosberg A Y and Meller A 2010 Electrostatic focusing of unlabeled DNA into nanoscale pores using a salt gradient *Nat. Nanotechnology* **5** 160–5
- [29] Luo K, Ala-Nissila T, Ying S-C and Bhattacharya A 2007 Influence of polymer-pore interactions on translocation *Phys. Rev. Lett.* **99** 148102
- [30] Kim M J, Wanunu M, Bell D C and Meller A 2006 Rapid fabrication of uniformly sized nanopores and nanopore arrays for parallel DNA analysis *Adv. Mater.* **18** 3149–53